

INVESTIGATION OF STRUCTURAL MEMBERS WITH BASALT REBAR REINFORCEMENT AS AN EFFECTIVE ALTERNATIVE OF STANDARD STEEL REBAR

ELAVENIL S*, SARAVANAN S AND ROHITH REDDY

VIT University, Chennai, India

(Received 17 June, 2017; accepted 24 November, 2017)

Key words: BFRP, Basalt rebars, Flexural behavior, Strain, RCC, Bond

ABSTRACT

Objectives: This research deals with the study of the flexure behaviour of beams reinforced with Basalt bars in contrary with the steel bar reinforced beams and comparing the stress strain behaviour and strain characteristics.

Methods: Basalt bars commonly known as Basalt Fiber Reinforced Polymer (BFRP) is an innovative component, and hence the differences and limitations of their bondage with concrete in structural members in comparison with conventional steel reinforcement of RCC members are identified. The project presents some experimental results of research by considering a flexural member (beam), reinforced with basalt bars, in contrary with the nominal steel reinforced beams and testing under loading frame of 500 kN capacity. The two grades of concrete involved are M30/40, while the reinforcement are done with 8 mm diameter basalt rebars and subjected for flexural strength evaluation. The various deflection patterns and nature of crack formation has been illustrated. The results incorporate the difference in the load-deflection pattern of BFRP beams with that of nominal control beams with steel reinforcement.

Applications/Improvements: This approach of BFRP reinforced beams can be effectively used in severe exposure conditions like marine conditions and areas prone to acid attacks due to their improved durability and strength characteristics.

INTRODUCTION

Over the past 30 years, fiber reinforced polymer materials are being involved effectively in construction field. It is one of the main development which has occurred in the composites polymer industry in the recent years made from basalt rock which is currently available for making Basalt FRP bars (hereafter called BFRP bars). Basalt (solidified volcanic lava) is an igneous rock. Fiber can be extruded from molten basalt rock at diameters between 13 to 20 μ in a single stage process. The fiber production process is similar to the process used for the production of glass fiber. Basalt bars have

various advantages compared with that of normal steel and other composites used as reinforcement, such as glass GFRP (glass fiber) and CFRP (carbon fiber). The primary composition of basalt rock is in the form of various oxides, with silica-oxide being most abundant. The percentage of silica oxide is generally between 51% and 58% by mass.

Basalt primarily comprises minerals plagioclase, pyroxene and olivine. When heated at high temperature, basalt is capable of producing a natural nucleating agent, which plays a major role in the thermal stability of the material. This leads to increased volumetric integrity when compared

to other materials. The notable characteristics of BFRP are: (1) mechanical properties (a) High tensile strength - up to 2.9 Gpa (b) Young's modulus - upto 90 Gpa. (2) Chemically inert, acidic, alkaline states. (3) High thermal stability - effective in insulating, electrical and sound properties (4) less weight and reduced self-weight characteristics. (5) Low elastic - moduli when compared to other FRP composites and conventional steel. (Values provided based on various literature study, exact values are decided only by the manufacturer based on quality of materials involved in manufacturing) where, BFRP bar is 4 times lighter than steel reinforcement with equal strength characteristics, which significantly reduces transportation costs for shipping, loading and unloading, as well as operating expenses at the construction site. The design guideline used for fiber reinforced polymer including, glass is based on ACI 440 - 1R.

LITERATURE REVIEW

1. (Marek, *et al.*, 2013) has done preliminary studies on BFRP rebars by testing its tensile test by unique testing equipment and analyzing the type of failure of BFRP strands and incorporating it to the failure modes in structures. Studies on stress-strain behavior was studied which was noted to be linear and completely different from steel reinforced structures which is considered to be a major disadvantage as structures involving large plastic deformations cannot be made by this kind of reinforcement.

i. It discusses about the Load - deflection, cracking behavior and stress limitation under BFRP Reinforced beams.

ii. Different amounts of longitudinal reinforcement at bottom phase by 8 mm BFRP rebars is examined using M30/35 Grade.

iii. Modulus of elasticity from the stress - strain curve was determined and was compared with conventional steel reinforced beam samples and shown that the elastic moduli of BFRP was about 5-7% smaller.

iv. Along with nature of crack and failure pattern, the width of crack formed during periodic loading was studied and was found to be of a higher value when compared to the steel reinforced sections.

v. Based on loading pattern and failure criteria it was concluded that critical load carrying capacity was about 20-25% higher than conventional steel rebars.

2. (Ahmed and Farid, 2016) carried out investigation on concrete beams strengthened by Basalt rebars for their shear behavior by constructing 10 samples

of beams (L=2000 mm; c/s = 152 mm × 254 mm) reinforced along longitudinal direction alone without any transverse reinforcement by fixing the test variability in terms of different geometry and level of reinforcement. Further the results were checked for acceptance according to standard values as per American standard codes (ACI-440.1R-15) which proved to be conservative. Also it clearly states the validity of design codes for determining the concrete contribution in shear strength of BFRP reinforced concrete beams. Behaviors of these various groups were analyzed in terms of

(i) *Strain variations during loading in both concrete and rebars.*

(ii) *Deflection measurement at mid span during loading (LVDT).*

(iii) *Cracking loads and failure modes arising as a result of all these varied behaviors are thereby calculated.*

3. (Pouya and Anil, 2015) carried out tests on progressive deformation in concrete due to sustained loading is analyzed along with exposure to alkaline solution at high temperatures and the results were compared with the acceptable standard values as per American Concrete Institute (ACI). It has been analyzed that the creep rupture strength of BFRP rebars are comparatively lesser than their tensile strength, when compared to that of steel bars. The creep nature of BFRP rebars depends on its own fiber properties, resin and their bonding with each other.

4. (Ahmed, *et al.*, 2015) studied the factors of bonding strength and behavior of BFRP rebars in concrete. The test was based on pull out mechanism and the test results were incorporated with that of GFRP rebars. The bonding nature was compared with many parameters like, Embedded length into concrete surface; Material of bars and elasticity & Diameter of bars. Although BFRP and GFRP showed almost the same bond-slip curves, BFRP rebars showed an average of 75% increased bonding capacity than GFRP. The bonding behavior of BFRP rebars were studied based on (a) embedded length (b) modulus of elasticity (c) bar diameter, and was concluded by experimental verification that the bonding nature varied inversely in all the three parameters considered.

PRELIMINARY RESULTS

Material Properties

BFRP rebars and steel rebars: The sample of specimen used for study is shown in (Fig. 1) and

Table 1 gives comparison of material properties of BFRP and Steel rods involved.

Cement and aggregates: The various material properties of the aggregates and cement involved are shown in Table 2.

Concrete mix design: The mix proportion for M30 and M40 Grade concrete mix is listed in Table 3 which is arrived from trial mix and their corresponding cement content. Mix proportion is denoted by Cement: Fine Aggregate: Coarse Aggregate: Water.

Fresh concrete properties: Workability is one of the important properties of fresh concrete, which is, directly or indirectly responsible for quality of concrete as a whole. Adequate workability on one hand improves the desirable properties of concrete such as, finishing, degree of compaction and strength, etc. (Punmia, 2007). The fresh concrete properties of both concrete grades of M30 and M40 mix are shown in Table 4.



Fig. 1 BFRP rebars of 8 mm diameter.

Table 1. Material properties of BFRP and steel

Characteristics	Steel bar	BFRP bars
Material	Steel	Basalt fiber roving with polymer
Tensile strength (Mpa)	400	1210 MPa
Elastic modulus	200000 MPa	59.3 GPa
Lengthening %	>14	2.7%
Heat Conductivity w/ m ² -°C	58	0.35
Thermal Expansion -10 ⁻⁶ / °C	13-15	Vertical - (9-12) Lateral - (21-22)
Density (t/m ³)	7.850	1.9 - 2.1
Corrosion stability	Corrode	Non-corrodable
Electrical conductivity	Conductor	Dielectric
Heat conductivity	Calorific	Non - calorific
Length	Core 4-20mm	As per requirement

Table 2. Preliminary test results on raw materials

Properties	F.A	C.A	Cement	Steel rod	BFRP
Specific Gravity	2.2	2.73	3.10	-	-
Consistency	-	-	32%	-	-
Initial and Final Setting Time	-	-	28 min and 550 min	-	-
Yield Strength of 8 mm rods (N/Mm ²)	-	-	-	465.1	1210
Uniformity Coefficient	2.8	-	-	-	-
Soundness Test	-	-	3.5	-	-

Table 3. Mix design details

Type of Mix	M 30	M 40
Mix proportion	1:1.43:2.31:0.40	1:1.24:2.10:0.35
Cement content	465 kg/m ³	514 kg/m ³
Fine aggregate	665 kg/m ³ (4.75 mm passing)	639.32 kg/m ³ (4.75 mm passing)
Coarse aggregate	1077 kg/m ³ (20 mm sized)	1080.30 kg/m ³ (20 mm sized)
Water	186 l/m ³	180 l/m ³

Table 4. Slump cone test details

S. No	Concrete Grade	Slump (Mm)
1.	M 30	10
2.	M 40	8

Table 5. Compressive strength details of M30 concrete cubes

Trial	Compressive Strength N/mm ²		
1.	23.15	28.80	37.60
2.	21.91	27.46	37.20
3.	22.35	29.82	37.40
Average	22.47	28.69	37.40

Table 6. Compressive strength details of M40 concrete cubes

Trial	Compressive Strength N/mm ²		
1.	25.82	40.1	43.95
2.	23.80	40.5	44.88
3.	26.80	39.02	43.95
Average	25.47	39.87	44.26

Hardened Concrete Properties

Compressive strength: Test results for conventional concrete grade of M30 and M40 mix for 7th, 14th and 28th day curing period are tabulated in Table 5 and 6.

Split tensile strength: Split Test results for conventional concrete grade of M30 and M40 mix for 7th, 14th and 28th day curing period are tabulated in Table 7.

Table 7. Split tensile strength details of M30 and M40 concrete cubes

Days of Curing	Split Tensile Strength N/mm ²	
	M30	M40
7 Days	2.26	2.68
14 Days	2.40	2.83
28 Days	2.83	2.82

Table 8. Elastic moduli values of M30 & M40 concrete cylinders

Days of Curing	Split Tensile Strength N/mm ²	
	M30	M40
7 Days	19771.06	21052.03
14 Days	20817.44	21838
28 Days	23281.81	26130.98

Modulus of Elasticity

The function of stress to strain ratio namely modulus of elasticity value are shown in Table 8.

EXPERIMENTAL INVESTIGATION

Design and Detailing of Beam Specimen as Per Code IS 456:2000

The test specimen consists of a beam portion of cross-section 150 mm × 200 mm. The length of the portion is 1.05 m (IS 456:2000).

Design Data

- Clear Span = 1.05 m
- Width of the support = 0.3 m
- Eff. span = 1.35 m
- Live Load = 5 kN/m

(As per design loading conditions IS 875-part 2)

- Compressive strength of concrete = 30 N/mm²
- Yield strength of steel = 415 N/mm²

Load considerations

Dead load = $0.150 \times 0.200 \times 25 = 0.75$ kN/m

Live load = 5 kN/m (min. criteria for beams)

As per (IS875 - Part-3)

Total Load (W) = 5.75 kN/m

Factored Load (W_u) = $1.5 \times 5.75 = 8.625$ kN/m

Reinforcement detailing and c/s of structure

The detailing of reinforcement along compression and tension side involves 2 no.s of 8 mm diabar respectively. The placing of steel and BFRP bars depends on the geometries assigned for the various specimens under M30 and M40 grade of concrete.

The stirrups are made of 6 mm diasteel bars at 150 mm spacing along its length.

(Fig. 2) shows the L/S of the beam specimen and (Fig. 3) shows the C/S detailing.

Geometric Specifications of Beam Specimen

The beam specimens were casted in the following combinations of steel and BFRP reinforced sections as shown in Table 9.

Casting of Specimens

The reinforcement bars of GFRP bars and Steel bars were terminated based on the design and the required cut lengths. Formwork for the beam was made using plywood mould as shown in the (Fig. 4). Also, the barbending of steel and BFRP rebars are shown in (Fig. 5).

The details of casting on M30 and M40 series of specimens are shown in (Fig. 6(a) and 6(b)).

Test Devices

A three Linear Variable Differential Transducers (LVDT) was installed along the 1/3rd of the simple span of beam to monitor the deflection of the load point of beam. The strains were measured over sequence of load by means of dumec gauge. The experimental beams with nominal length of 1050 mm were loaded by two point loading arrangement separated by a distance of 300 mm apart between loading points. Supports at the soffit is given by

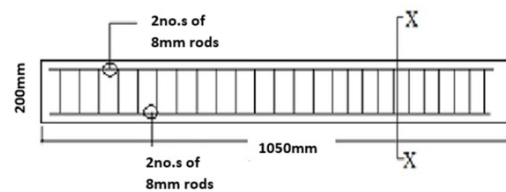


Fig. 2 L/s of the beam specimen.

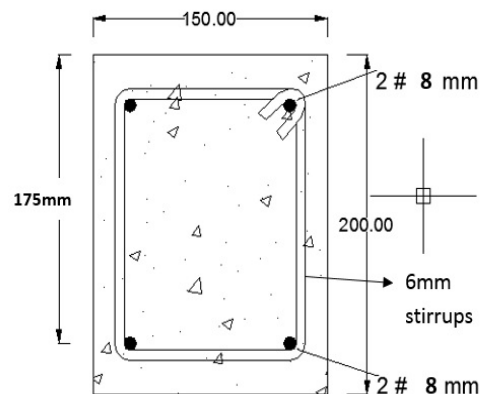


Fig. 3 C/s of the beam specimen (S/C-X-X).

Table 9. Geometrical combinations of beam samples

Beam Designation	Top Reinforcement	Bottom Reinforcement	Stirrups (steel)
B 30	2# 8 mm steel	2# 8 mm steel	6 mm#150 mm
B 30 - 1	2# 8 mm BFRP	2# 8 mm BFRP	6 mm#150 mm
B 30 - 2	2# 8 mm steel	2# 8 mm BFRP	6 mm#150 mm
B 40	2# 8 mm steel	2# 8 mm steel	6 mm#150 mm
B 40 - 1	2# 8 mm BFRP	2# 8 mm BFRP	6 mm#150 mm
B 40 - 2	2# 8 mm steel	2# 8 mm BFRP	6 mm#150 mm



Fig. 4 Formworks for the proposed beam specimens.



Fig. 5 Barbending of the proposed beams (BFRP & Steel).



Fig. 6 (a) Casting of M30 series of beams.



Fig. 6 (b) Casting of M40 series of beams.

knife edged roller supports. (Fig. 7(a) and 7(b)) shows the spacing details and the actual setup of the tested specimen respectively. The load applied over beam was around 5 kN and after each increment the evolution of beam specimen behaviour is inspected over concerning several parameters like, deflection, strain which was recorded and then analyzed (Douglas and Amir, 2015).

PRELIMINARY RESULTS

The tests on the casted specimens and its comparison

with that of the control beams are categorized with their corresponding test results.

Behaviour of Beam

Basically the behaviour of the beam is examined based on the loading criteria in which ultimate load plays a vital role. The formation of first crack was analyzed by studying the load deflection curves. The average of initial cracking load of beam and the series of B30/B40 are tabulated. The corresponding load upon cracking is directly related to tensile strength which, is a function of its compressive strength.

Mode of Failure

The load corresponding to initial crack formation and ultimate failure along with various modes of failure for each specimen tested is shown in Table 10. The control beam, exhibited flexure by yielding of steel bars denoted by (F.F), while crushing of concrete denoted as (C.C) was the predominant mode of failure. Tension failure in the BFRP reinforcement was noted by rebar rupture at the point of maximum bending moment. Thus the composite beam of BFRP and steel fails by rupture (B.R).

Deflection Behaviour of Beam

M30 series of specimens: The load to mid-span deflection and ultimate loads causing failure of the steel, BFRP and compositely reinforced concrete beams with grade of M30 are shown in Table 11 and the corresponding variations are presented in (Fig. 8).

The actual formation of initial and final cracks on the M30 specimen upon loading is shown in (Fig. 9).

M40 series of specimens: Bilinear curves were seen for all beams with BFRP reinforcement and show lesser deflection in compositely reinforced beam compared over the beam reinforced with full BFRP. Table 12 represents the load - deflection behaviour and ultimate loads causing failure of the steel, BFRP and compositely reinforced concrete beams with grade of M40 and the corresponding variations are shown in (Fig. 10).

The actual formation of initial and final cracks on the M40 specimen upon loading is shown in (Fig. 11).

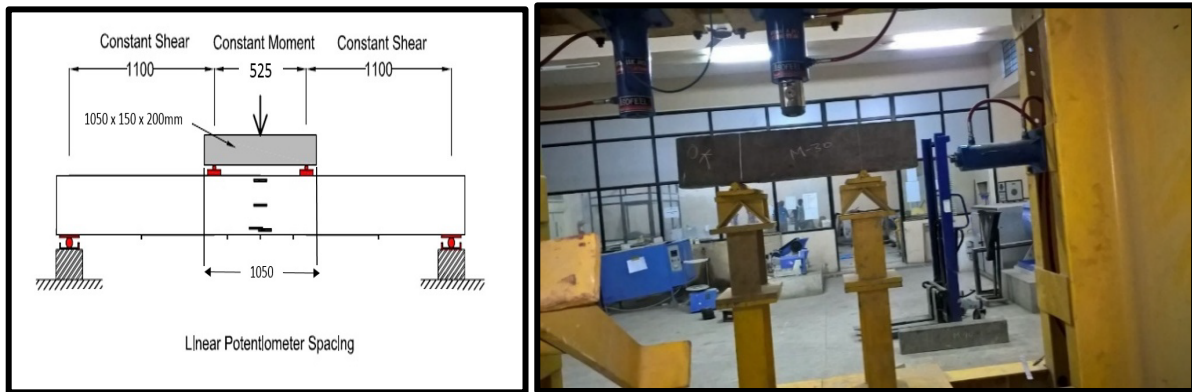


Fig. 7 (a and b) Experimental setup.

Table 10. Loading results and failure modes

Beam Series	Cracking Load (kN)	Ultimate Load (kN)	Failure Mode
B30*	32	95	F.F
B30-8B8B	32	140	C.C
B30-8S8B	32	160	B.R
B40*	34	108	F.F
B40-8B8B	32	156	C.C
B40-8S8B	40	180	B.R

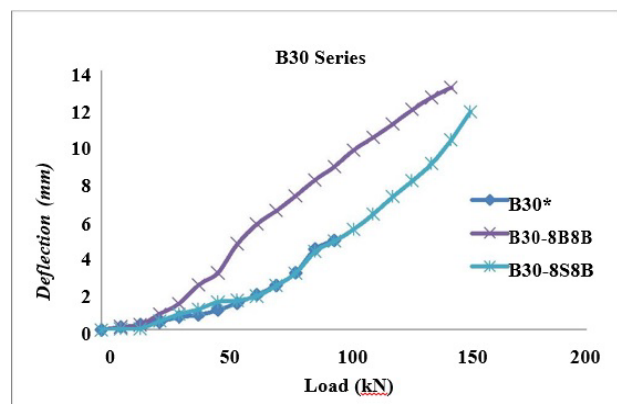


Fig. 8 Load vs. deflection in M30 series of beams.

Table 11. Loading-deflection behavior – M30 series

Load (kN)	Deflection (mm)		
	B30*	B30-8B8B	B30-8S8B
0	0	0	0
8	0.14	0.17	0.05
16	0.28	0.27	0.06
24	0.43	0.85	0.48
32	0.7	1.42	0.85
40	0.81	2.42	1.11
48	1.07	3.07	1.52
56	1.45	4.65	1.59
64	1.89	5.71	1.82
72	2.4	6.44	2.39
80	3.08	7.23	3.06
88	4.36	8.1	4.23
96	4.84	8.82	4.79
104	--	9.72	5.43
112	--	10.4	6.25
120	--	11.12	7.2
128	--	11.91	8.05
136	--	12.56	8.97
144	--	13.1	10.27
152	--	--	11.78

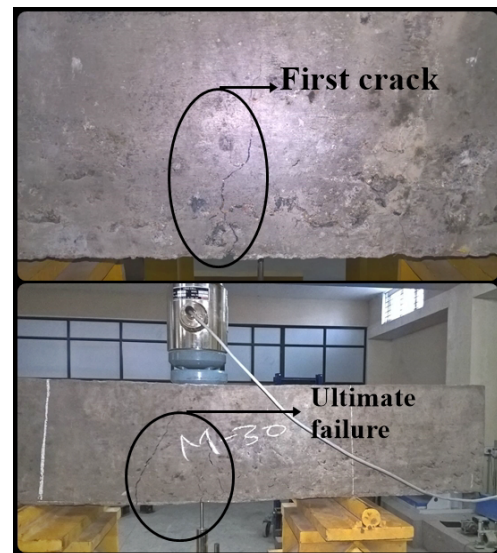


Fig. 9 Initial and final crack formation in M30 beam specimen.

Strain behaviour: A typical plot of the load and corresponding concrete strain relation for the beam specimen of concrete grade M30 is shown in (Fig. 12) and the corresponding values are tabulated in Table 13. Initial linear path of strain distribution is evident,

while totally 3 consecutive strain behaviour for the tested specimens were formed with similar nature. The cracking of beam specimen occurs and their strain differences among them increases rapidly. Strain over beam section is calculated by load increment of 5 kN.

Table 12. Loading-Deflection behavior – M40 series

Load (kN)	Deflection (mm)		
	B40*	B40-8B8B	B40-8S8B
0	0	0	0
8	0.09	0.12	0.06
16	0.22	0.27	0.17
24	0.4	0.56	0.31
32	0.72	0.9	0.5
40	1.01	1.42	0.79
48	1.43	1.83	1.21
56	1.73	2.49	1.57
64	2.03	2.88	1.82
72	2.33	3.65	2.11
80	2.62	4.13	2.4
88	2.91	4.83	2.69
96	3.42	5.34	2.97
104	4.02	5.87	3.27
112	5.22	7.17	3.64
120	6.81	9.23	3.83
128	8.69	10.19	4.39
136	--	11.21	4.88
144	--	12.34	5.72
152	--	13.97	6.45
160	--	15.19	7.12
168	--	--	7.88
176	--	--	9.28
184	--	--	9.98

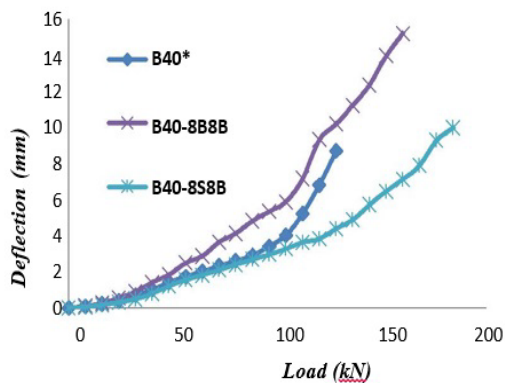


Fig. 10 Load vs. deflection in M40 series of beams.

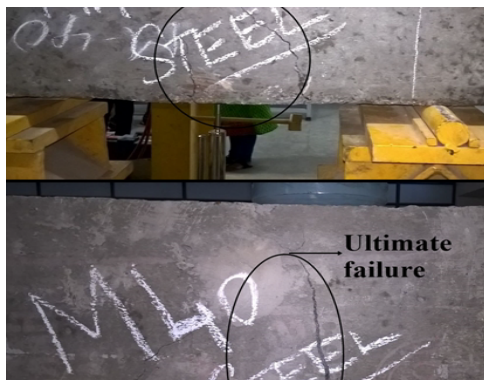


Fig. 11 Initial and final crack formation in M40 beam specimen.

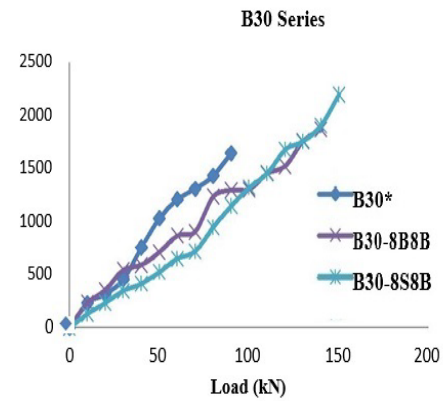


Fig. 12 Strain distribution in M30 series of beams.

Table 13. Concrete strains – M30 series

Load (kN)	Concrete Strains		
	B30*	B30-8B8B	B30-8S8B
0	0	0	0
10	234	234	130
20	315	356	234
30	456	546	350
40	756	590	415
50	1030	712	525
60	1209	867	650
70	1309	904	720
80	1432	1234	945
90	1645	1297	1145
100	--	1302	1320
110	--	1456	1452
120	--	1523	1680
130	--	1759	1754
140	--	1870	1905
150	--	--	2195

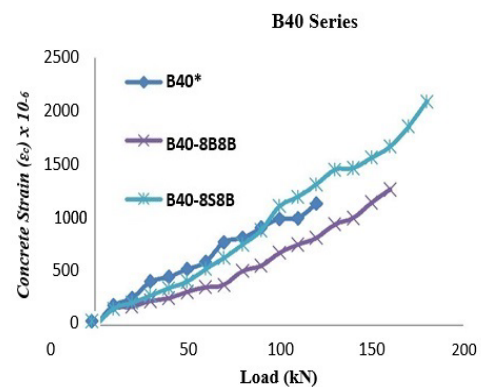


Fig. 13 Strain distribution in M40 series of beams.

Where, strain from demec gauge is calculated from top and bottom zone of beam with a gauge length of 200 mm from which average strain is calculated and plotted over the load.

Table 14. Concrete strains - M40 series

Load (kN)	Concrete strains		
	B40*	B40-8B8B	B40-8S8B
0	0	0	0
10	189	156	156
20	256	178	215
30	412	230	280
40	456	256	350
50	530	315	415
60	595	360	530
70	780	380	632
80	820	512	756
90	915	560	890
100	998	680	1115
110	1003	756	1202
120	1140	819	1318
130	--	947	1456
140	--	1004	1470
150	--	1150	1569
160	--	1270	1670
170	--	--	1860
180	--	--	2090

(Fig. 13) represents the concrete strain of the steel bars, BFRP bars and composite reinforced concrete beams with grade of M40 are presented. Table 14 represents the concrete strain of the steel bars; BFRP bars and composite reinforced concrete beams with grade of M40.

CONCLUSION

1. Tests were conducted for 6 no.s of BFRP reinforced concrete beams and their flexural strength behaviour and concrete strains were tested and their percentage effectiveness was studied.
2. From experimental study, it is observed that the beam specimen of M30 grade reinforced with BFRP bars has increased flexural behaviour up to 23% and load carrying capacity up to 12% and beam specimen with both BFRP and steel showed increased flexure strength up to 27% and load carrying capacity up to 15% in comparison with control beams of the same grade.
3. Similarly the beam specimens of M40 grade reinforced with BFRP bars has increased flexural behaviour up to 19% and load carrying capacity up to 6.7% and beam specimen with both BFRP and steel showed increased flexure strength up to 25% and load carrying capacity up to 11.8% in comparison with control beams of the same grade.
4. Also it is observed that the beam specimens of M30 grade reinforced with BFRP bars carried a maximum load of 145 kN and that reinforced with

both BFRP and steel up to 160 kN. Similarly beams specimens of M40 grade reinforced with full BFRP bars carried up to 156 kN and that of both steel and BFRP up to 180 kN.

5. Since, BFRP bars offer high strength performance and a steel bar offers a good ductility which in composite is observed that it has good behaviour in overall parameters taken in account like, load-deflection behaviour, strain distribution, failure mode and crack pattern which results in a better behaviour over control beam samples.
6. The concrete strain behaviour was maximum in beam specimens reinforced with both BFRP and steel in composite, M30 grade specimens showed increased strain value of 9.5% and that of M40 grade was 21%.

ACKNOWLEDGEMENTS

Authors are most grateful and wish to thank the University of VIT Chennai, and the department of Structural Engineering for providing moral support and guidance all through the project for completing the research work.

REFERENCES

- (IS 456:2000) Plain and reinforced concrete code of practice. Design of beams.
- Ahmed, E.R. and Farid, A. (2016). Concrete contribution to shear strength of beams reinforced with basalt fiber-reinforced bars. *Journal of Composites for Construction*. 20(4) : 04015082.
- Ahmed, E.R., Mohamed-Amine, A. and Radhouane, M. (2015). Bond performance of basalt fiber-reinforced polymer bars to concrete. *Journal of Composites for Construction*. 19(3) : 04014050.
- Douglas, T. and Amir, F. (2015). Performance of concrete beams reinforced with basalt FRP for flexure and shear. *Journal of Composites for Construction*. 19.
- Marek, U., Andrzej, L. and Andrzej, G. (2013). Investigation on concrete beams reinforced with basalt rebars as an effective alternative of conventional R/C structures. *Procedia Engineering*. 57 : 1183-1191.
- Pouya, B. and Anil, P. (2015). Creep ruptures performance of basalt fiber-reinforced polymer bars. *Journal of Aerospace Engineering*. 28(3) : 04014074.
- Punmia, B.C. (2007). Text book of design of RC structures by limit state design.